Journal of Neurochemistry

JOURNAL OF NEUROCHEMISTRY | 2015 | 133 | 284–297 doi: 10.1111/jnc.12979

ORIGINAL ARTICLE

Differential effects of lipopolysaccharide on energy metabolism in murine microglial N9 and cholinergic SN56 neuronal cells

Joanna Klimaszewska-Łata,* Sylwia Gul-Hinc,* Hanna Bielarczyk,* Anna Ronowska,* Marlena Zyśk,* Katarzyna Grużewska,* Tadeusz Pawełczyk† and Andrzej Szutowicz*

*Department of Laboratory Medicine, Medical University of Gdańsk, Gdańsk, Poland

†Department of Molecular Medicine, Medical University of Gdańsk, Gdańsk, Poland

Abstract

There are significant differences between acetyl-CoA and ATP levels, enzymes of acetyl-CoA metabolism, and toll-like receptor 4 contents in non-activated microglial N9 and non-differentiated cholinergic SN56 neuroblastoma cells. Exposition of N9 cells to lipopolysaccharide caused concentration-dependent several-fold increases of nitrogen oxide synthesis, accompanied by inhibition of pyruvate dehydrogenase complex, aconitase, and α-ketoglutarate dehydrogenase complex activities, and by nearly proportional depletion of acetyl-CoA, but by relatively smaller losses in ATP content and cell viability (about 5%). On the contrary, SN56 cells appeared to be insensitive to direct exposition to high concentration of lipopolysaccharide. However, exogenous nitric oxide resulted in marked inhibition pyruvate dehydrogenase and aconitase activities, depletion of acetyl-CoA, along with respective loss of SN56 cells viability. These data indicate that these two common neurodegenerative signals may differentially affect energy-acetyl-CoA metabolism in microglial and cholinergic neuronal cell compartments in the brain. Moreover, microglial cells appeared to be more resistant than neuronal cells to acetyl-CoA and ATP depletion evoked by these neurodegenerative conditions. Together, these data indicate that differential susceptibility of microglia and cholinergic neuronal cells to neurotoxic signals may result from differences in densities of toll-like receptors and degree of disequilibrium between acetyl-CoA provision in mitochondria and its utilization for energy production and acetylation reactions in each particular group of cells.

Keywords: acetyl-CoA, cytotoxicity, lipopolysaccharide, N9 cells, NO, SN56 cells.

J. Neurochem. (2015) **133**, 284–297.

Inhibition of brain energy metabolism, accompanied by inflammatory activation of microglial cells is a characteristic feature of several neurodegenerative brain diseases, including Alzheimer's (AD), Wernicke, aluminum, or vascular encephalopathies. Glutamatergic-excitotoxic stimulation is a commonly recognized early pathogenic signal, triggering subsequent late neurodegenerative events. These pathologic conditions were found to induce inflammatory activation of microglia, including increased synthesis of nitric oxide (NO) yielding peroxynitrite radicals, as well as the release of several pro- and anti-inflammatory cytokines such as interleukins-1β, IL-6 (interleukins-1β, IL-6), or tumor necrosis factor-α (TNFα) (Cunningham 2013; Welser-Alves and Milner 2013). Cytokines, depending on their concentrations in perisynaptic compartments of the brain, may exert either neuroprotective or neurotoxic effects. They may also combine with primary neurotoxic signals, aggravating course of neurodegeneration (Block *et al.* 2007).

Received June 25, 2014; revised manuscript received October 10, 2014; accepted October 13, 2014.

Address correspondence and reprint requests to Andrzej Szutowicz, Department of Laboratory Medicine, Medical University of Gdańsk, ul. Dębinki 7 bldg. 27, 80-211 Gdańsk, Poland. E-mail: aszut@gumed.edu.pl.

Abbreviations used: ACh, acetylcholine; AD, Alzheimer's disease; cAMP, dibutyryl cyclic AMP; ChAT, choline acetyltransferase; IL-1β, interleukin-1β; IL-6, interleukin-6; KDHC, α-ketoglutarate dehydrogenase complex; LPS, lipopolysaccharide; MEM-FBS, Minimum Eagle's Medium with 10% fetal bovine serum; NAA, N-acetyl-L-aspartate; NGF, nerve growth factor; NO, nitric oxide; PDHC, pyruvate dehydrogenase complex; SNP, sodium nitroprusside; TLR, toll-like receptor; TNF-α, tumor necrosis factor-α.

Brain cholinergic neurons were found to be particularly prone to neurotoxic conditions because of relative shortage of acetyl-CoA in their mitochondrial compartments (Szutowicz *et al.* 2013; for review). Such conditions, specific for cholinergic neurons, could result from competition for acetyl-CoA between energy producing and acetylcholine (ACh) synthesizing pathways (Szutowicz *et al.* 2013). That leads to early disturbances in cholinergic neurotransmission, in the form of activation of non-quantal and inhibition of quantal ACh release (Szutowicz *et al.* 1999; Jankowska-Kulawy *et al.* 2010). These findings remain in line with studies on AD patients, which revealed correlations between cognitive deficits before death and losses in cholinergic markers found in *post-mortem* brains (Bierer *et al.* 1995; Pappas *et al.* 2000). Moreover, those alterations paralleled deficits of several enzymes of tricarboxylic acid cycle (TCA) in affected areas of cerebral cortex of autopsied AD brains (Bubber *et al.* 2005). In line with these findings, positron emission tomography studies have demonstrated inhibition of ^{18}F-deoxy-glucose uptake and decreases in ATP and phosphocreatine levels in brains of AD patients (Klunk *et al.* 2004). However, whole-brain models of inflammation are not capable of demonstrating putative differential alterations in energy metabolism that likely occur in diverse neuronal and glial compartments during the course of neurodegenerative processes.

Diverse studies have revealed that several neurotoxic signals, including excess or aberrant distribution of Zn, Al, NO, or amyloid-β, as well as thiamine pyrophosphate deficiency, are capable of direct inhibition of pyruvate dehydrogenase (PDHC), ketoglutarate dehydrogenase α-ketoglutarate dehydrogenase complex (KDHC), and some other TCA enzyme activities in whole brain, nerve terminals, and cholinergic SN56 neuronal cells of septal origin (Moncada and Bolanos 2006; Sensi *et al.*2009; Szutowicz *et al.* 2013). These conditions were found to bring about deficits of acetyl-CoA both in mitochondrial and cytoplasmic compartments (Szutowicz *et al.* 2013). Detrimental effects were more pronounced in neurons with high expression of the cholinergic phenotype, than in non-cholinergic ones, and correlated well with losses of ACh-dependent transmitter functions and their viability (Szutowicz *et al.* 2004; Bielarczyk *et al.* 2005). These alterations in cellular model of cholinergic encephalopathy correlated with losses of enzymes of energy metabolism and cholinergic markers in human brain cortex regions affected by AD pathology (Bubber *et al.* 2005; Szutowicz *et al.* 2006, 2013).

Microglia are a group of brain cells that quickly responds to several pathologic conditions with proliferation, phagocytosis, burst of NO/peroxynitrite, and pro-inflammatory cytokines that become harmful to adjacent neuronal cells. Several studies indicate that microglial inflammatory response to xenobiotics and endogenous signals may contribute to neuronal degeneration through excessive production of NO and a vast range of pro-inflammatory cytokines (Gibbons and Dragunow 2006; Block *et al.* 2007; Brown and Neher 2010, 2014). For instance, such responses have been observed in primary and clonal microglial cultured cells, upon their exposition to bacterial lipopolysaccharide (LPS) (Nakamura *et al.* 1999; Hines *et al.* 2013). The toll-like surface receptors (TLR) in microglial cells were found to be responsible for their several cytotoxic activities evoked by LPS-containing pathogens (Block *et al.* 2007; Okun *et al.* 2011; Zhao *et al.* 2014).

Also, LPS-evoked excessive synthesis of NO could be harmful not only for adjacent neurons but also for producing microglial cells. It has been shown that in BV-2 microglial cells, LPS caused inhibition of oxygen consumption, respiratory chain complex activities, and suppression of ATP levels, which were prevented by NO-synthase inhibitors (Moss and Bates 2001; Chénais *et al.* 2002). However, there is no evidence to prove whether these alterations are linked to respective disturbances in provision of acetyl-CoA.

Studies of human autopsy brains have revealed that neurodegeneration is accompanied by declines in activities of several enzymes of energy and acetyl-CoA metabolism (Sheu *et al.* 1985; Bubber *et al.* 2004, 2005) There are also data demonstrating that both primary and clonal cholinergic brain-derived neuronal cells, when differentiated with dibutyryl cyclic AMP (cAMP), retinoic acid, or nerve growth factor (NGF) toward mature cholinergic phenotype, became more susceptible to different neurotoxic/excitotoxic signals, including NO excess, because of decreased availability of acetyl-CoA in their mitochondrial compartments, caused by its utilization of ACh synthesis (Olesen *et al.* 1998; Szutowicz *et al.* 2004, 2006, 2013).

It has been also demonstrated that LPS activates microglia through alterations in a broad range of gene expression yielding excessive synthesis of neurotoxic oxygen/peroxynitrite radicals and release of pro-inflammatory cytokines (Xie *et al.* 2002; Liu and Hong 2003; McKimmie *et al.* 2006). It is also not known whether LPS may directly affect key parameters of energy and acetyl-CoA metabolism in neuronal cells expressing cholinergic phenotype. That could shed new light on inflammation-linked mechanism(s) of preferential vulnerability of brain cholinergic neurons taking place during the course of AD and other dementia types (Maccioni *et al.* 2009). So far, neither *in vivo* positron emission tomography nor whole brain *post-mortem* studies provide information on distribution parameters of acetyl-CoA and energy metabolism among different types of neuronal and non-neuronal compartments of the brain under neurodegenerative conditions. Therefore, the aim of this study was to investigate whether and how LPS, and its key mediator NO, may differentially affect energy and acetyl-CoA metabolism of microglial and cholinergic neuronal cells.

Materials and methods

Reagents

Unless otherwise specified growth media, and other biochemicals were obtained from Sigma–Aldrich (Poznań, Poland).

Cell cultures

Microglial N9 cells between 19th and 39th passage were seeded at a density of 40 000 cells/cm^2 on 75 cm^2 Falcon vessels in Minimum Eagle's Medium with 10% inactivated fetal bovine serum containing 1.0 mmol/L L-glutamine, 0.05 mg of streptomycin, and 50 U of penicillin per 1 mL and cultured for 48 h, as described above. Then medium was replaced with the experimental one containing different concentrations of LPS as indicated, and culture continued for next 24 h.

SN56.B5.G4 cholinergic murine neuroblastoma cells, with stable expression of PDHC and choline acetyltransferase (ChAT) between 22nd and 40th passage, were used for experiments (Hammond *et al.* 1990; Blusztajn *et al.* 1992; Szutowicz *et al.* 1999). Cells were seeded at a density of 40 000 cells/cm^2 on 75 cm^2 Falcon vessels in Minimum Eagle's Medium with 10% fetal bovine serum supplemented with 1.0 mmol/L L-glutamine, 0.05 mg of streptomycin, and 50 U of penicillin per 1 mL. Cells were grown at 37°C in atmosphere 5% CO_2, 95% air. Cholinergic differentiation was induced by the addition of 1 mmol/L dibutyryl cAMP (cAMP) for 48 h. At this time, growth media were replaced by the experimental ones containing no differentiating agent, without or with LPS (1 μg/mL), and culture was continued for the next 24 h.

Cells that remained attached to the plate were harvested into 10 mL of ice-cold solution containing 140 mmol/L NaCl, 5 mmol/L KCl, 1.7 mmol/L NaK-Pi buffer (pH 7.4), 5 mmol/L glucose and collected by centrifugation at 200 *g* for 7 min. Washing medium was removed and cells were suspended in 320 mmol/L sucrose containing 10 mmol/L HEPES buffer (pH 7.4) to obtain protein concentration 10.0 mg/mL. Immediately after collection, cells specimens were taken for trypan blue exclusion assay and for metabolic studies. For ChAT and PDHC assays, cell specimens were kept frozen at −20°C for 2–7 days. Remaining enzyme activities were assessed in unfrozen samples within 24 h after the cells were harvested.

Trypan blue exclusion assay

Cell suspension was mixed with equal volume of 0.4% isotonic trypan blue solution. Total cell number and fraction of non-viable, dye accumulating cells were counted after 2 min in Fuchs–Rosenthal hemocytometer under light microscope (Spector *et al.*1998).

Metabolic studies

Depolarizing incubation medium contained in a final volume of 1.0 mL 2.5 mmol/L pyruvate, 2.5 mmol/L L-malate, 90 mmol/L NaCl, 30 mmol/L KCl, 20 mmol/L NaHEPES (pH 7.4), 1.5 mmol/L Na-Pi, 0.32 mmol/L sucrose, and 0.7–1.0 mg of cell protein. Incubation was started by the addition of cell suspension and continued for 30 min at 37°C with shaking at 100 cycles per min. For determination of total acetyl-CoA content, 0.3 mL of incubation medium was centrifuged at 5000 *g* for 2 min. Supernatant was removed and cell pellet was deproteinized as indicated below (Szutowicz *et al.* 2004).

Acetyl-CoA assay

To assess the whole-cell acetyl-CoA content, the cell pellet was deproteinized by suspension in a small volume of 5 mmol/L HCl and incubation in a boiling bath for 1 min. Extracts were treated with maleic anhydride solution in ethyl ether for 2 h to remove CoA-SH. Cycling reaction was carried for 60 min in 0.1 mL of medium containing 1.9 mmol/L acetyl phosphate, 1.2 mmol/L oxaloacetate, 1.0 IU phosphotransacetylase, and 0.12 U citrate synthase. Cycling reaction was stopped by heating samples at 100°C for 10 min and citrate formed was determined (Szutowicz and Bielarczyk 1987).

Enzyme assays

Immediately before the assay, samples were diluted to a desired protein concentration in 0.2% v/v Triton X-100. ChAT (acetyl-CoA:choline-O-acetyltransferase, EC 2.3.1.6) activity was assessed by the radiometric method using [1-14C]acetyl-CoA as a substrate (Fonnum 1975). Pyruvate dehydrogenase complex (pyruvate:lipoate oxidoreductase acceptor acetylating) was assayed by the citrate synthase coupled method (Szutowicz *et al.* 1981). Activities of citrate synthase (EC 2.3.3.1), aconitase [citrate(isocitrate) hydro lyase, EC 4.2.1.3], NADP isocitrate dehydrogenase [threo-D-isocitrate:NADP oxidoreductase (decarboxylating) EC 1.1.1.42], α-ketoglutarate dehydrogenase complex, ATP-citrate lyase (acetyl-CoA:oxaloacetate C-acetyltransferase [(pro-S)carboxymethyl forming, ADP phosphorylating], EC 2.3.3.8), and carnitine acetyltransferase (acetyl-CoA:carnitine *O*-acetyltransferase, EC 2.3.1.7) were assayed by the methods listed elsewhere (Jankowska-Kulawy *et al.* 2010; Ronowska *et al.* 2010). All enzymes were assayed at 37°C.

Direct effects of LPS, sodium nitroprusside (SNP) or lipoamide on enzyme activities in Triton-lysed homogenates were tested by sample pre-incubation at 37°C, in respective assay media, for 15 min before starting the assay.

ATP and N-acetylaspartate (NAA) assays

For ATP/N-acetyl-L-aspartate (NAA) assessment, cells were cultured on 3-cm-diameter plates under various experimental conditions (see Cell cultures). The media were withdrawn, cells on the plates were gently washed with ice-cold-buffered saline containing 5 mmol/L glucose, deproteinized with 1.0 mL 4% $HClO_4$, and harvested into plastic tubes in ice. Protein was removed by centrifugation for 60 s at 5000 *g* and clear supernatant after neutralization with K_2CO_3 was used for ATP determination by luminometric method (Gorman *et al.* 2003) using Berthold Junior LB 9509 luminometer (Berthold Technology. Bad-Wilbad, Germany). For modified NAA assay (Koller *et al.* 1984), neutralized samples were passed through 0.22-μm polytetrafluoroethylene (PTFE) Cronus filter and loaded (90 μL) onto ODS-80TM C-18 C, 250 × 4.6 mm, 5 μm particle size column provided with its own guard column (Tosoh Bioscience, Tokyo, Japan) and connected to an HPLC apparatus consisting of a Series 200 autosampler, pump system, vacuum degasser, and diode array detector (Perkin Elmer, Warsaw, Poland). The mobile phase contained 0.1% phosphoric acid and 0.5% methanol (a flow rate 0.8 mL/min). Elution peak for NAA detected at 210 nm had retention time 7 min 30 s. and was identical with that of standards.

Protein assay

Protein was assayed by the method of Bradford (1976) with human immunoglobulin as a standard. Perchloric acid precipitated samples were dissolved in 0.2 mol/L potassium hydroxide (KOH) before the assay.

Cytokine and TLR4 assays

The levels of IL6, and TNF-α in the culture media were assayed using commercial Platinum ELISA kits (eBioscience, Bender MedSystems GmbH, Vienna, Austria). Levels of TLR4 in lysed cell homogenates were determined using ELISA kit (MyBioSource, San Diego, CA, USA).

Statistics

Statistical analyses were carried out using Graph Pad Prism 4 programme (Graph Pad Software, San Diego, CA USA) by one-way ANOVA with Bonferroni multiple comparison test or by non-paired Student's *t*-test, at $p < 0.05$ being considered statistically significant.

Results

Cell growth rates

During entire 72-h culture, N9 cell number increased 3.7-fold, whereas that of SN56 2.5-fold, respectively, reaching confluent conditions. On the other hand, during 48–72 h subconfluent experimental step both cell lines displayed similar 25% daily growth rates.

Parameters of acetyl-CoA and energy metabolism in native SN56 cholinergic and N9 microglial cells

In SN56 cholinergic neuronal cells, activities of key energy metabolism regulatory enzymes PDHC and KDHC were about 1.5 and 2 times higher than those in microglial N9 cells, respectively (Table 1). Also, aconitase activity was 50% higher in neuronal cells. Activities of ATP-citrate lyase and L-carnitine acetyltransferase, enzymes involved in the indirect transport of acetyl groups from mitochondria to cytoplasm in SN56, were found to be 2.8 and 6.8 times, respectively, higher than those in N9 cells. Accordingly, ATP content in SN56 cells was found to be two times higher than that in the microglia. Microglia contained no NAA, whereas high levels of this metabolite were found in SN56 cells (Table 1). Also, ChAT activity was found to be present in SN56 cells only. On the contrary, whole SN56 acetyl-CoA content appeared to be 34% lower than that in the whole N9 microglia. Low neuronal acetyl-CoA level was confined to cytoplasm, where it was found to be 44% lower than that in the cytoplasmic compartment of microglia. On the other hand, mitochondrial acetyl-CoA levels appeared to be similar in both cell lines (Table 1). N9 cells displayed nine times greater levels of TLR4, than SN56 (Table 1).

Effects of LPS and SNP on morphology of N9 microglial and cholinergic SN56 cells

In control conditions, majority of N9 microglia displayed uniform round shape with small fraction of elongated cells. Low 0.01 μg/mL LPS concentration caused no apparent changes in N9 morphology (Fig. 1b), but small, although significant, increase of non-viable cell fraction from about 2–4% (Fig. 2b). At higher, 0.1–10.0 μg/mL concentrations of LPS, the 20–30% fraction of N9 cells, of larger size, ameboid shape, with plasma membrane blebs-like deformations, as well as vacuoles and dense granulations located in cytoplasm, were observed (Fig. 1c–e). However, fraction of

Table 1 Differences in parameters of acetyl-CoA and energy metabolism between non-modified microglial N9 and non-modified neuronal cholinergic SN56 cells

Parameter	Value in microglial N9 cells	Value in cholinergic neuronal SN56 cells
Pyruvate dehydrogenase complex (nmol/min/mg protein)	5.7 ± 0.3	8.4 ± 0.3*
Citrate synthase (nmol/min/mg protein)	192 ± 4	125 ± 17*
Aconitase (nmol/min/mg protein)	21.5 ± 1.5	33.3 ± 3.5*
Isocitrate dehydrogenase NADP (nmol/min/mg protein)	39.0 ± 2.2	19.6 ± 0.6*
α-ketoglutarate dehydrogenase complex (nmol/min/mg protein)	2.1 ± 0.2	4.1 ± 0.3*
ATP-citrate lyase (nmol/min/mg protein)	5.6 ± 0.4	38.4 ± 1.4*
Carnitine acetyltransferase (nmol/min/mg protein)	5.3 ± 0.3	14.7 ± 0.7*
Choline acetyltransferase (nmol/min/mg protein)	n.d.	0.12 ± 0.008
Toll-like receptor 4 (ng/mg protein)	1.08 ± 0.20	0.12 ± 0.05*
Whole cell acetyl-CoA level (pmol/mg protein)	42.5 ± 2.1	28.3 ± 0.9*
Mitochondrial acetyl-CoA (pmol/mg protein)	8.0 ± 2.0	8.8 ± 0.7
Cytoplasmic acetyl-CoA (pmol/mg protein)	34.5 ± 2.0	19.5 ± 0.7*
Whole-cell N-acetyl-L-aspartate level (nmol/mg protein)	n.d.	69.5 ± 1.4
Whole cell ATP level (nmol/mg protein)	11.7 ± 0.8	23.5 ± 2.3*
Mitochondrial protein (% of total)	49.4 ± 1.7	51.8 ± 1.6

Data are means ± SEM from 3 to 15 experiments. Significantly different from respective N9 values: *$p < 0.001$.
n.d., non-detectable.

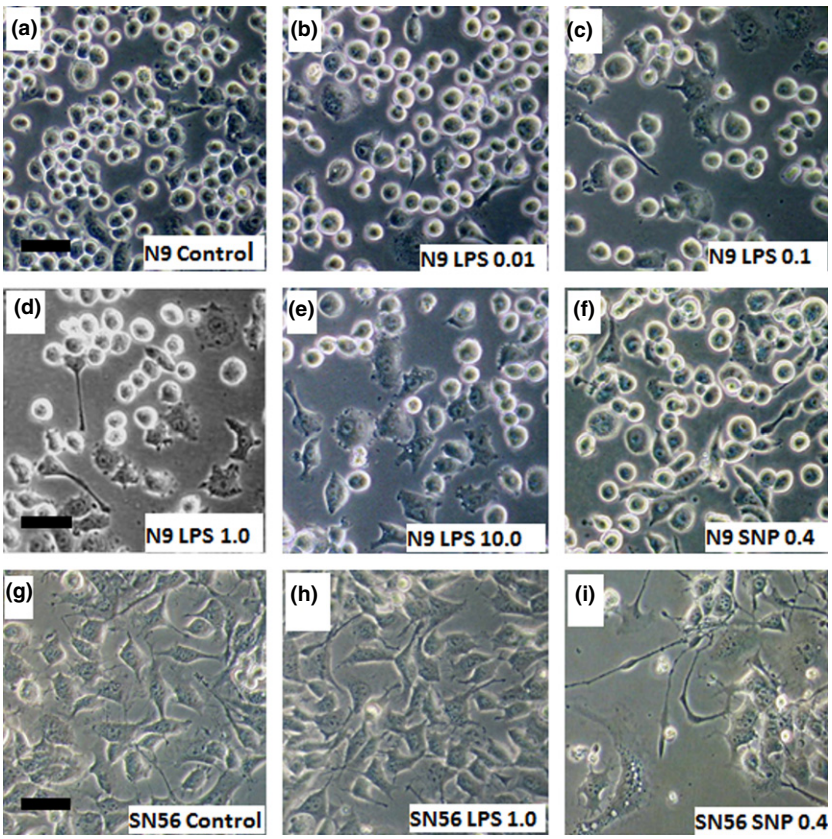

Fig. 1 Alterations in N9 microglial cell morphology upon 24-h exposition to: (a) control without additions; (b) lipopolysaccharide (LPS) 0.01 μg/mL; (c) LPS 0.1 μg/mL; (d) LPS 1.0 μg/mL; E. LPS 10.0 μg/mL, (f) sodium nitroprusside (SNP) 0.4 mmol/L. Alterations in morphology of SN56 cholinergic neuroblastoma cells. (g) control without additions; (h) LPS 1.0 μg/mL, (i) SNP 0.4 mmol/L. Scale bars equal to 10 μm. Photos are characteristic for 3–10 experiments.

non-viable, trypan blue-retaining, cells increased modestly to 8% only despite 1000-fold elevation of LPS level (Fig. 2b and e). Also, long-term exposure to exogenous NO, generated by SNP, modified neither morphology nor viability of N9 microglia (Fig. 1a and f).

Cholinergic non-differentiated SN56 neuronal cells demonstrated typical ramified morphology with synaptic-like connections (Fig. 1g). Addition of 1.0 μg/mL LPS to the culture medium changed neither neuronal morphology nor their viability (Fig. 1h, 4b). On the contrary, exogenous NO brought about neuronal cell disruption with granular and vacuolar type of degeneration (Fig. 1i).

Concentration-dependent effects of LPS on energy metabolism and viability of microglial N9 cells

Exposition of N9 cells to LPS brought about concentration-dependent increase in NO_2, accumulation in the culture medium, which displayed biphasic kinetics, apparently corresponding to its high and low-affinity putative binding sites of half activation concentrations of 3 μg/mL and 14.7 μg LPS/mL, respectively(Fig. 2a). These alterations in NO synthesis were accompanied by respective biphasic elevations in fraction of, trypan blue retaining N9 cell that reached 8.5% at 10 μg/mL LPS concentration in the culture medium (Fig. 2b). Highly significant positive correlation existed between LPS concentration-dependent increases of non-viable N9 cell fraction and rates of NO_2 accumulation ($r = 0.934$, $p = 0.002$) (Fig. 2c).

LPS in 0.1 μg/mL concentration increased TNF-α and IL-6 synthesis/release by N9 microglia by about 20 and 91 times, respectively (Fig. 2d). On other hand, in SN56 cells culture, 1.0 μg/mL LPS caused no significant alterations in their TNF-α and IL-6 levels (not shown).

LPS-evoked alterations in N9 viability, described above, coexisted with its inhibitory effects on PDHC, aconitase, and KDHC activities *in situ*. For each of tested enzymes, LPS concentration-dependent suppression plots displayed biphasic shape with apparently high sensitivity to low (up to about 0.01 μg/mL) and low sensitivity to high (up to 10 μg/mL) LPS concentrations, respectively (Fig. 3a–c). KDHC in N9 appeared to be the most susceptible to chronic suppressive effects of LPS with half inhibitory concentration- [IC_{50}] of 0.0065 μg/mL (Fig 3c). PDHC and aconitase were found to be more resistant to this treatment with high-affinity [IC_{50}] values of 0.041 and 0.140 μg LPS/mL (Fig. 3a and b), respectively. None of Dixon's plots for higher, 0.1–10.0 μg/mL LPS concentrations, displayed level of statistical significance (not shown). In addition, LPS in concentrations up to 10 μg/mL caused no significant inhibition in activities of NADP-isocitrate dehydrogenase (ICDH-NADP) and ATP-citrate lyase within N9 cells (Fig. 3d) as well as citrate synthase and carnitine acetyltransferase (not shown).

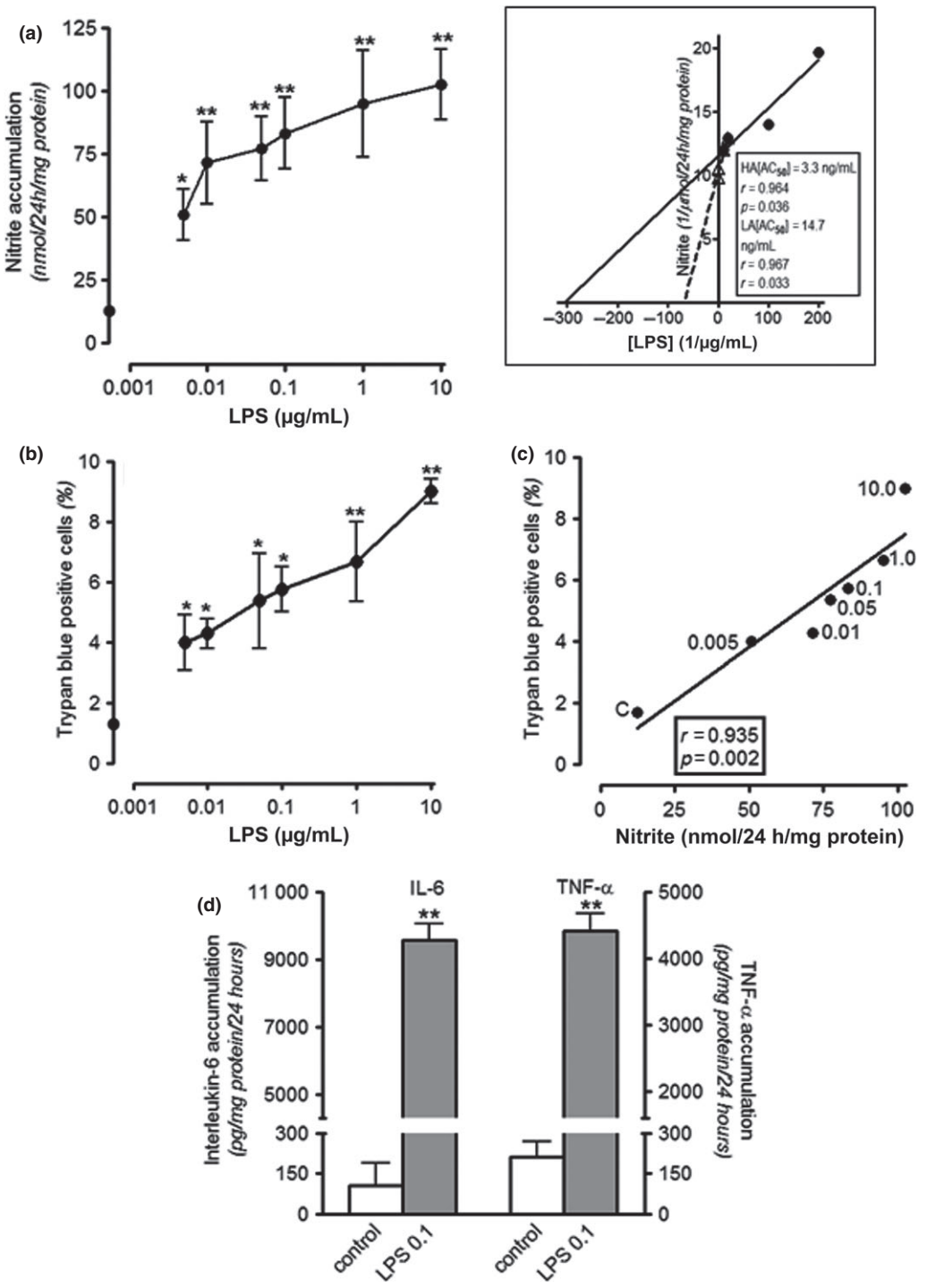

Fig. 2 Concentration-dependent long-term 24-h effects of lipopolysaccharide (LPS) on N9 microglial cells: (a) nitric oxide (NO) synthesis/release, direct and (box) double reciprocal plots of LPS-dependent activation of NO synthesis assayed as nitrite accumulation; (b) non-viable cell fraction; (c) correlation plot between non-viable, trypan blue positive, cell fraction, and NO (nitrite) accumulation rate (numbers indicate LPS concentrations). (d) effects of LPS on interleukin-6 and tumor necrosis factor-α (TNF-α) accumulation rates in the growth medium. Data are means ± SEM from 3 to 15 experiments. Significantly different from respective no addition values: $*p < 0.01$; $**p < 0.001$.

LPS-evoked *in situ* inhibition in enzyme activities was accompanied by concentration-dependent suppressions in whole-cell acetyl-CoA and ATP contents, at similar [IC_{50}] values of 0.17 and 0.20 μg/mL, respectively (Fig. 3e and f). Levels of these metabolites, at 0.1 μg/mL LPS in the medium, fell down to 57% and 64% of control values,

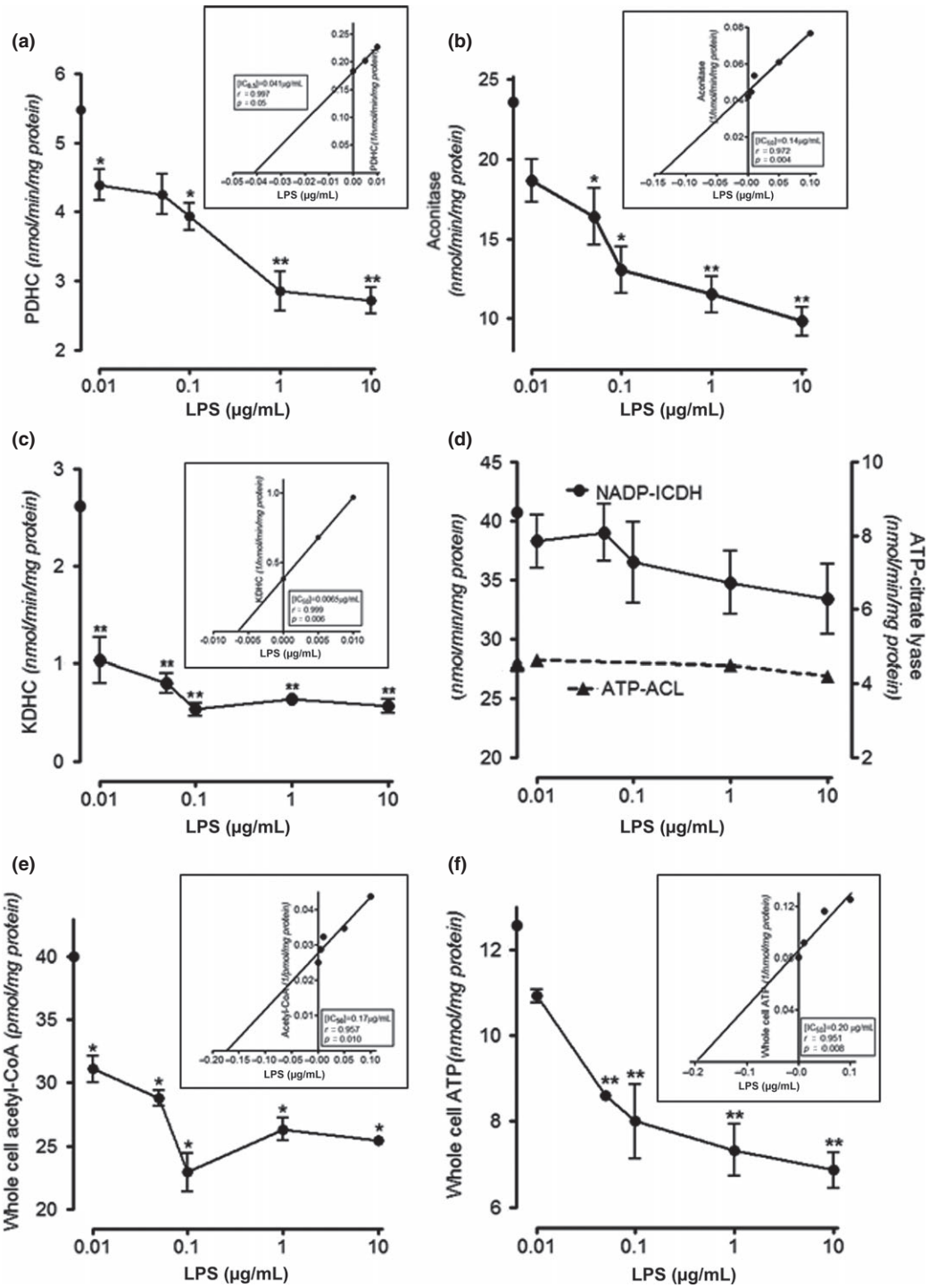

Fig. 3 Concentration-dependent effects of 24-h exposition of N9 microglial cells to lipopolysaccharide (LPS): (a) pyruvate dehydrogenase complex (PDHC) activity; (b) aconitase activity; (c) α-ketoglutarate dehydrogenase complex (KDHC) activity; (d) NADP-isocitrate dehydrogenase (ICDH-NADP), ATP-citrate lyase (ATP-ACL) activities; (e) whole-cell acetyl-CoA levels; (f) whole-cell ATP levels. Boxes present Dixon's plots of given enzyme activity or metabolite level against LPS concentration. Data are means ± SEM from 3 to 12 experiments. Significantly different from no LPS controls: $*p < 0.05$, $**p < 0.001$.

respectively (Fig. 3e and f). Further elevation of LPS in the medium to 10 μg/mL caused none or relatively small augmentation of these inhibitory effects (Fig. 3e and f). In consequence, LPS concentration-dependent decreases in ATP content in N9 microglia correlated with those in acetyl-CoA levels ($r = 0.908$, $p = 0.012$).

Also small, but statistically significant, LPS concentration-dependent increases of non-viable fraction of N9 cells displayed inverse correlations with decreasing PDHC ($r = 0.947$, $p = 0.002$) and aconitase activities ($r = 0.929$, $p = 0.003$) but relatively weak one with alterations of KDHC activity ($r = 0.813$, $p = 0.029$) (Table 2). Highly significant correlations were also found to exist between LPS concentration-dependent alterations in N9 cells viability and acetyl-CoA ($r = 0.933$, $p = 0.006$) or ATP levels ($r = 0.952$, $p = 0.003$), respectively (Table 2). These suppressive modifications in PDHC, aconitase, and KDHC activities, as well as in acetyl-CoA and ATP levels also correlated significantly with LPS-induced increases in rates of NO_2 accumulation (Table 2).

Differential effects of LPS and NO excess on microglial N9 and cholinergic SN56 neuroblastoma cells

Exposition of N9 to LPS (0.01 μg/L) caused 4-fold increase in rate of NO synthesis, to about 15 μmol/24 h/L of the growth medium (Fig. 4a) accompanied by a small but reproducible elevation in fractional content of non-viable cells from 2% to 4% (Fig. 4b). Also, the addition of 0.4 mmol/L SNP, generating exogenous NO in similar amounts of 16 μmol/24 h/L growth medium, caused similar small loss of N9 viability. Combined use of these compounds yielded additive effect of 6% fraction of non-viable N9 cells accompanied by a further rise in NO production. (Fig. 4a and b).

Exposition to LPS (0.01 μg/L) decreased PDHC, and aconitase activities and suppressed acetyl-CoA level in N9 cells by 28%, 67%, and 43%, respectively (Fig. 4c–e). Exogenous, SNP-generated NO either alone or in combination with LPS, caused over 50% suppression of PDHC, but no alterations in aconitase activities and acetyl-CoA content (Fig 4c–e).

On the contrary, exposition of SN56 cholinergic cells to 100 times higher, 1.0 μg/mL LPS concentration brought about no alterations in their viability and residual synthesis of endogenous NO (Fig. 4a and b). Also, no alterations in activities of those enzymes and acetyl-CoA content were found (Fig. 4c–e).

On the other hand, exposition of SN56 cholinergic neuronal cells to 0.4 mmol/L SNP increased NO levels in growth medium, yielding elevation of their non-viable fraction up to 25% (Fig. 4a and b). These detrimental effects of SNP in SN56 cells were accompanied by 30%, 83%, and 39% decreases in their PDHC, aconitase activities, and acetyl-CoA contents, respectively (Fig. 4c–e). LPS partially overcame the effects of SNP on SN56 cell viability and their aconitase activity (Fig. 4b and d). On the other hand, LPS augmented suppressive effects of SNP on PDHC and acetyl-CoA to 43% and 90%, respectively (Fig. 4c and e).

Table 2 Correlations between enzymatic and metabolic parameters of energy metabolism and NO synthesis and viability of N9 microglial cells

	NO synthesis (Nitrite accumulation)		Loss of viability (Trypan blue-positive cells)	
Enzyme/metabolite	*r*	*p*	*r*	*p*
PDHC	−0.923	0.003	−0.947	0.002
Aconitase	−0.941	0.0015	−0.929	0.003
KDHC	−0.971	0.0003	−0.813	0.029
Acetyl-CoA	−0.968	0.0004	−0.933	0.006
ATP	−0.999	<0.0001	−0.952	0.003

Calculated from data presented in Figs 2 and 3.

Direct effects of LPS and SNP on PDHC and aconitase activities

Inhibition of PDHC and aconitase activities *in situ* within cells exposed to LPS could result either from direct or indirect/adaptative reactions to endogenous NO or LPS itself (Figs 3 and 4). To clarify this point, direct effects of these compounds on enzyme activities in cell homogenates have been investigated. Hence, LPS in 1.0 μg/L concentration altered neither PDHC nor aconitase activities in homogenates of N9 microglial cells (Table 3). On the other hand, in these conditions SNP inhibited those enzymes for about 45% (Table 3). Pre-treatment of homogenates with lipoamide partially protected microglial PDHC, but not aconitase against SNP-induced inhibition. Also, in homogenates of SN56 cells, LPS had no effect on PDHC and aconitase activities, whereas SNP exerted 80% and 63% inhibition, respectively. Lipoamide pre-treatment resulted in partial protection of neuronal PDHC, but failed to protect aconitase against SNP inhibition (Table 3).

Discussion

Alterations in cell growth rate are factors that may variably affect levels of different parameters of energy production and synthetic pathways utilizing acetyl-CoA in each type of cultured cells. Therefore, in this work, N9 and SN6 cells have been seeded in densities, which assured reaching subconfluency after 48-h culture. At this time point, differences in any parameter of acetyl-CoA and energy metabolism in either N9 or SN56 could result from variations in their intrinsic properties or specific functions, but not from differences in their growth rates.

It is known that cAMP, retinoic acid, or NGF/BDNF (brain-derived neurotrophic factor) might interfere with LPS-linked signaling and energy metabolism pathways in microglial and neuronal cells, respectively (Szutowicz *et al.* 1999, 2004; Schubert *et al.* 2001; Jin *et al.* 2014). Therefore, neither cell line used here was subjected to any agent

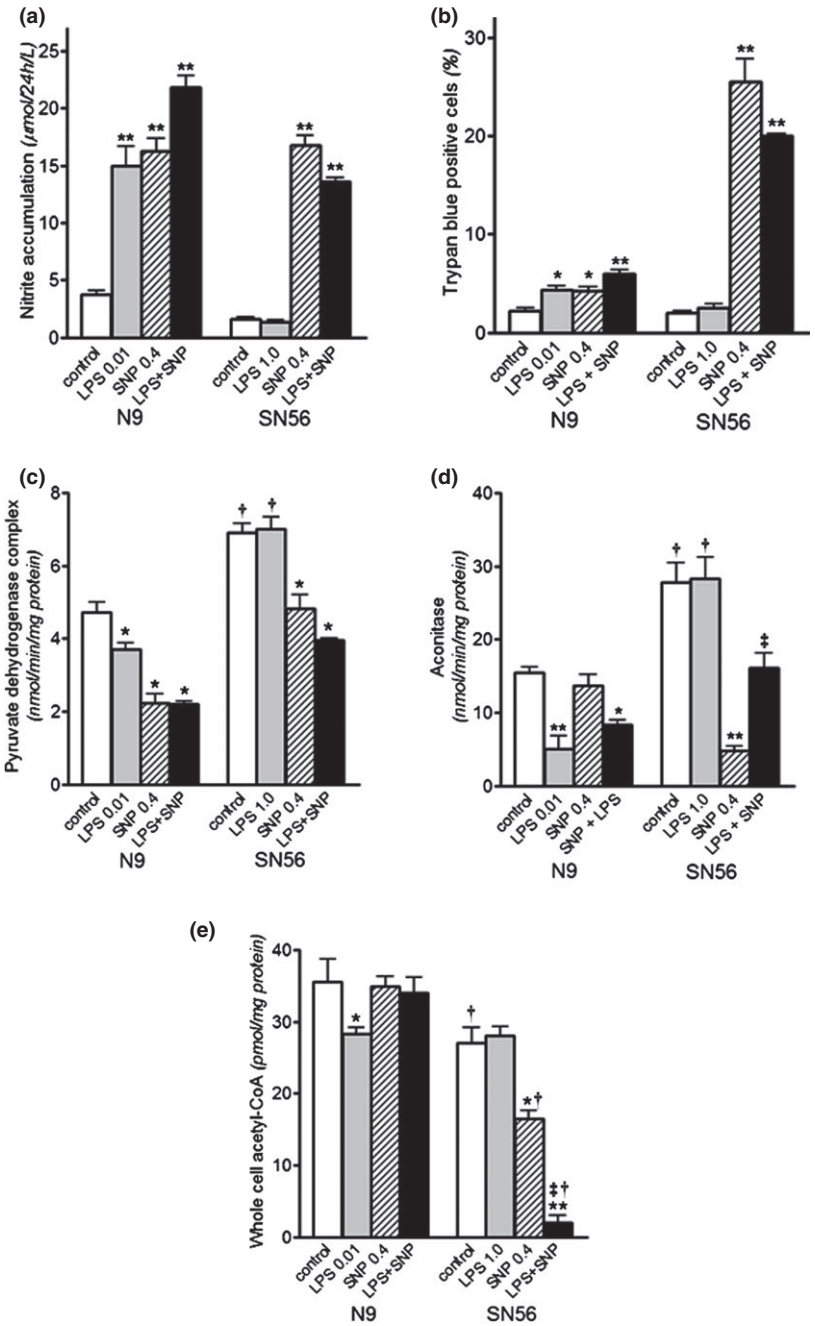

Fig. 4 Differential, long-term 24-h effects of 0.01 μg/mL lipopolysaccharide (LPS) on microglial N9 cells and 1.0 μg/mL LPS on cholinergic SN56 neuronal cells. Sodium nitroprusside (SNP) 0.4 mmol/L was used in both cultures. Effects on: (a) Nitrite accumulation rates; (b) Cell viability, (c) pyruvate dehydrogenase complex (PDHC) activity; (d) aconitase activity; (e) Whole-cell acetyl-CoA level. Data are means ± SEM from 4 to 15 experiments. Significantly different from: respective control, $^{*}p < 0.05$, $^{**}p < 0.001$; respective SNP 0.4 mmol/L, $^{\ddagger}p < 0.01$; respective N9 cells, $^{\dagger}p < 0.01$.

modifying their native phenotypes. As a result, non-differentiated SN56 neuronal cells displayed relatively low levels of cholinergic phenotype as compared with cAMP/retinoic acid/NGF differentiated ones (Table 1) (Szutowicz *et al.* 2004, 2006, 2013). Despite that, they were capable of synthesizing, maintaining and releasing ACh in quantal mode, with rates comparable with those seen in brain synaptosomal preparations (Ronowska *et al.* 2010; Szutowicz *et al.* 1998, 2004; Tomaszewicz *et al.* 2003). Also, ChAT activity in non-differentiated SN56 appeared to be either comparable or several times higher than those in other cholinergic cell lines (Table 1) (Kalisch *et al.* 2002; Olesen *et al.* 1998; Machova *et al.* 2006; Szutowicz *et al.* 1999, 2004, 2006). Therefore, the expression of cholinergic phenotype non-modified SN56 cells appeared to be high enough for comparative studies with non-cholinergic cells such as microglia (Table 1, Fig. 4).

Past studies investigating physiological and pathological alterations of energy metabolism in whole-brain preparations were not capable of demonstrating differential compartmentalization of acetyl-CoA and energy metabolism intermediates in diverse groups of brain cells, which may be of key

Table 3 Direct inhibitory effects of LPS and SNP on activities of PDHC and aconitase in homogenates of N9 microglial cells

	PDHC	Aconitase	PDHC	Aconitase
	N9 microglial cells homogenates		SN56 neuronal cells homogenates	
Additions	Fraction of control activity (%)			
Lipoamide 0.1 mmol/L	98.4 ± 2.0	95.9 ± 8.2	97.7 ± 6.6	90.4 ± 2.2
LPS 1.0 μg/mL	92.6 ± 4.1	102.7 ± 4.1	90.1 ± 3.4	88.6 ± 3.3
SNP 0.4 mmol/L	55.3 ± 3.8**	53.7 ± 2.0*	19.3 ± 5.0**†	37.2 ± 0.6**†
Lipoamide + SNP	78.2 ± 1.9*‡	61.2 ± 2.1*	38.5 ± 3.5**†‡	37.9 ± 1.6**†

For absolute values corresponding to 100% controls, see data in Table 1. Data are means ± SEM from 3 to 11 experiments. Significantly different from: respective control, *$p < 0.01$, **$p < 0.001$; respective relative value in N9 cell homogenate, †$p < 0.005$, respective value at 0.4 mmol/L SNP alone, ‡$p < 0.05$.

significance for their individual susceptibility to pathological conditions (Table 1) (Reynolds and Blass 1975; Tuček1993; Szutowicz *et al.* 1996, 2006, 2013; Gibbons and Dragunow 2006; Chen *et al.* 2012).

In this study, higher activities of PDHC, aconitase, and KDHC in SN56 cholinergic than in N9 microglial cells (Table 1) appear to be compatible with greater demands for energy in the former ones because of their neurotransmitter functions. It is also known that ATP-citrate lyase and carnitine acetyltransferase constitute pathways involved in indirect transport of acetyl moieties from mitochondrial to cytoplasmic compartment in cholinergic neurons (Bielarczyk and Szutowicz 1989; Szutowicz *et al.* 1996). High activities of ATP-citrate lyase and carnitine acetyltransferase in SN56 neuronal cells remain in accordance with their high demand for efficient transport of acetyl units for cytoplasmic ACh synthesis (Table 1) (Szutowicz *et al.* 1996, 2013). On the other hand, relatively low levels of acetyl-CoA in cytoplasmic compartment of SN56 might result from its consumption for ACh synthesis (Table. 1) (Szutowicz *et al.* 2006, 2013). Another neuron-specific pathway lowering overall content of acetyl-CoA in SN56 could be the synthesis of N-acetyl-L-aspartate in their mitochondria (Table 1) (Baslow 2007 for review). On the contrary, relatively high levels of ATP found in SN56 cells would be compatible with their higher activities of PDHC and KDHC than in N9, which are rate-limiting steps for acetyl-CoA synthesis and its metabolic flux through the TCA cycle, respectively (Table 1).

In microglial N9 cells, slower than in neuronal SN56 cells, metabolic flux through TCA cycle would yield lower content of ATP (Table 1). Thus, the brain microglia should be considered as the brain cellular compartment containing low activities of enzymes of energy metabolism and levels of ATP and relatively high levels of acetyl-CoA, respectively (Table 1, Fig. 4c–e).

Several-fold higher levels of TLR4 in N9 than in SN56 cells would explain their greater responsiveness to LPS (Table 1, Fig. 4). Functional competence of TLR4 pathway in N9 cells was demonstrated here by several fold, LPS-induced increases in release rates of NO, IL-6, and TNF-α (Fig. 2a and d). Their absolute values were of similar range as those reported by others for N9 and BV2 microglial cells (Dodd and Filipov 2011; Ye *et al.* 2013). They were also found to be comparable with rates of those cytokine release reported earlier for primary microglia and whole-brain studies (Lu *et al.* 2010; Welser-Alves and Milner 2013). Therefore, these N9 cells may be an appropriate model for studying alterations in energy metabolism taking place in brain microglial compartment *in situ,* under inflammatory conditions.

Different enzymologic and metabolic alterations in N9 cells following their chronic exposition to LPS were of adaptative character (Table 1, Fig. 2). They took place in the cells which preserved their structural integrity at highest LPS levels till the end of culture (Fig. 1a–e, 2b). N9 cells gradually changed their basal resting round shape to ameboid one upon exposition to increasing concentrations of LPS (Fig. 2a–e), as reported earlier (Lu *et al.* 2010). They also preserved up to 95% viability, as estimated by trypan blue exclusion assay at pathophysiologically relevant concentrations of LPS (Fig. 1b and c, 2b, 4b). These findings remain in accord with, earlier studies demonstrating NO-evoked morphological alterations in microglial mitochondria, reflecting increased energy consumption (Banati *et al.* 2004). Apparently, adaptative, activatory responses of N9 cells to LPS, may result from activation of TLR4 and presumably other TLR surface receptors, without significantly compromising their viability (Table 1, Figs 2a, b, d, 4a and b) (Brown and Neher 2010, 2014; Okun *et al.* 2011).

On the other hand, control cholinergic SN56 control cells demonstrated ramified shapes with apparent intercellular connections (Fig. 1h). Insensitivity of SN56 to LPS may be caused by several times lower than in N9, expression of TLR4 (Table 1). There was demonstrated here by lack of activation NO synthesis by SN56 exposed to LPS. (Figs 1g and h, 4a). That might explain absence of any suppressive effects of LPS

on viability and energy metabolism in SN56 cells (Fig. 4b–e). It may be presumably due to TLR2-dependent up-regulation of calpastatin, being neuroprotective for neuronal cells (Chen *et al.* 2012; Vaisid and Kosower 2013). Such small or none responses to LPS were also reported for brain dopaminergic and hippocampal neuronal cells (Beynon *et al.* 2013; Zhao *et al.* 2014). Our data are also compatible with earlier reports showing no expression of surface TLR4 in human NB-I neuroblastoma cells yielding their unresponsiveness to LPS (Table 1, Fig. 4) (Hassan *et al.* 2006). These data are compatible with reports showing no activation of NFκB (nuclear factor kappa-light-chain-enhancer of activated B cells), TRIF (TIR-domain-containing adapter-inducing interferon-β), or JNK (c-Jun N-terminal kinase) pathways in LPS-exposed neurons (Okun *et al.* 2011).

Functional competence of non-differentiated cholinergic SN56 cells have been confirmed in past by their ability for synthesis and K/Ca-dependent quantal release of ACh with rates comparable to those found in brain synaptosomal fraction (Blusztajn *et al.* 1992; Szutowicz *et al.* 1999, 2004, 2013). Therefore, presented here alterations parameters of acetyl-CoA metabolism in NO-exposed or LPS/NO-treated, cholinergic SN56 cells may decently reflect changes taking place in the cholinergic compartment under excitotoxic/inflammatory conditions in the brain (Fig. 4a–e) (Bubber *et al.* 2005; Cunningham 2013; Szutowicz *et al.* 2013).

Strong activating effects of low LPS concentrations on microglial NO/cytokine synthesis could result from the presence of high density of high-affinity TLR4 receptors on their plasma membranes linked with the activation of *iNOS* (inducible nitric oxide synthase) and *TNF*-α genes (Table 1, Figs 2a and d, 4a) (Jung *et al.* 2005; Block *et al.* 2007; O'Neill and Hardie 2013). On the other hand, biphasic shape of LPS-induced viability and NO synthesis plots in N9 suggests the existence multiple classes of target proteins of high and low affinity to LPS, respectively (Fig. 3a and b) (Akashi *et al.* 2003; McKimmie *et al.* 2006). Hence, steep parts of inhibitory plots at low LPS concentrations may reflect activation of TRL-4 receptors, abundant both in primary and clonal microglial cells (Fig. 3a–c) (Akashi *et al.* 2003; Lehnardt *et al.* 2003). Indeed, values of half-maximal inhibition constant of LPS to KDHC equal to 6.5 ng/mL, appeared to be close to its high-affinity activation concentration for NO synthesis equal to 3.3 ng/mL (Figs 2a, 3c). Both of them were of the same range as functional affinity constant of LPS to MD2-TLR4 adapter protein on HEK293T cells, being in range of 0.7–7.5 ng/mL (recalculated from Visintin *et al.* 2001). It indicates that KDHC may be most sensitive target for endogenous NO-derived peroxynitrite, generated by activated microglia (Figs 2a, 3c). On the other hand, substantial suppression of PDHC and aconitase activities in N9 cells required higher rates of NO synthesis, attainable after stimulation of low-affinity cell surface, LPS-binding sites. (Figs 2a, 3a and b). Such properties of NO interactions with microglial enzymes could be the one of causes of relative resistance of microglial cells to endogenous, LPS-induced burst of NO. (Figs 2a and b, 3b and c).

The possibility of direct inhibition/inactivation of PDHC or aconitase by LPS has been excluded here on account of the absence of any direct effects of this pathogen on their activities in both N9 and SN56 cell homogenates (Table 3). Therefore, the excess of NO/peroxynitrite produced by LPS-activated microglia should be considered as an early endogenous signal leading to inhibition of above enzymes of energy metabolism (Figs 2a, 4a–d) (Szutowicz *et al.* 1998, 2013; Chénais *et al.* 2002). These results point to contribution of this phenomenon to the kind of poorly controlled mechanism, self-limiting excessive microglial reactivity/proliferation under inflammatory conditions in the brain (Park *et al.* 1999; Chénais *et al.* 2002). Such conclusion is supported by the fact that in intact N9 cells LPS caused dose-dependent elevation of endogenous NO synthesis, which strongly correlated with parallel inhibitions of PDHC, aconitase, and KDHC (Figs 2a and b, 3a–c, Table 2). In addition, strong direct correlation between loss of trypan blue excluding capacity and nitrite accumulation indicates that the latter may be a key factor inducing impairment of excessively activated microglial cells, through inhibition of key enzymes of acetyl-CoA metabolism (Figs 2a–c, 4c and d) (Nakamura *et al.* 1999; Gibbons and Dragunow 2006). The direct inhibition of these enzymes by endogenously produced NO/NOO^- could be an immediate cause of early deficits of acetyl-CoA and ATP in LPS-exposed microglia (Table 3, Fig. 3e and f). Such thesis is supported by the existence of significant inverse correlations between PDHC, KDHC aconitase activities, and acetyl-CoA/ATP levels and rates of NO_2 generation in LPS-treated N9 (Fig. 2a and b, 3a–c, Table 2). Also, direct inhibition of PDHC and aconitase in N9 cell homogenates by SNP-derived NOO^- confirms the existence of such mechanism basing upon LPS-NO-mediated effects on microglial cells in the brain *in situ* (Table 3, Fig. 4c and d). In addition, this finding remains in accord with past studies, demonstrating that exposition cultured microglial cells or isolated brain nerve terminals and mitochondria to SNP/NO brought about *in situ* inhibition of their PDHC, aconitase, and KDHC activities (Szutowicz *et al.* 1998, 2013; Park *et al.* 1999; Chénais *et al.* 2002; Bielarczyk *et al.* 2006). Thus, such mechanisms would explain appearance of LPS-evoked early deficits of acetyl-CoA and ATP in microglial cells, likewise in other classes of brain cells (Fig. 3e and f). These findings are compatible with reports on NO-evoked inhibition of several respiratory chain enzymes by excess of NO, in the LPS-exposed microglial cells (Chénais *et al.* 2002).

There is, however, disparity between strong inhibition of KDHC, PDHC, aconitase, and acetyl-CoA by burst of endogenous NOO^- and relatively small, < 10% loss of N9

microglia viability (Figs 3b, 4a–c). This may result from relatively small demand of N9 cells for energy and preservation ICDH-NADP activity (Fig. 3d). This enzyme was found to provide NADPH for maintenance proper level of intracellular GSH, effectively protecting microglia against nitrozative stress (Persson and Ronnback 2012). In addition, NOO^- did not inhibit ATP-citrate lyase, which supplies acetyl-CoA necessary for lipid synthesis in growing cells (Fig. 3d) (Zaidi *et al.* 2012).

On the other hand, LPS-TLR4 evoked elevations in IL-6, TNF-α, and other cytokines releases from N9 may also activate NO-independent cytotoxic signaling pathways decreasing their own and adjacent neuronal cells viability (Table 1, Fig. 2b) (Block *et al.* 2007; Cunningham 2013; Brown and Neher 2014). Such NO-independent effects were observed in cytokine-treated cholinergic SN56 cells (Szutowicz *et al.* 2004; Bielarczyk *et al.* 2005). Thus, also in microglial cells, cytokines might constitute complementary to NO signals contributing to acetyl-CoA and ATP deficits (Fig. 3e and f). These data suggest that decreased acetyl-CoA level may be a common executor for diverse cytotoxic signaling pathways, in different cellular compartments of the brain.

Presented data support the thesis that the same cytotoxic signal, like exogenous NO, may exert highly differential effects on viability of (micro) glial and neuronal (cholinergic) brain cells (Fig. 4a and b). One of the reasons for greater resistance of microglial cells to cytotoxic inputs could be their lower energy demand (Table 1). That would help microglia to sustain energy-suppressing effects caused by burst of endogenous NO/peroxynitrite during its activation by LPS, amyloid-β, or other neurodegenerative signals (Figs 2, 3, 4) (Chénais *et al.* 2002; Xie *et al.* 2002; Block *et al.* 2007; Cunningham 2013). Aconitase and acetyl-CoA in N9 were also not suppressed by exogenous NO (Fig. 4d and c). On the contrary, in SN56 cells those parameters were markedly reduced by exogenous NO, what remains in agreement with over 20% loss of their viability (Fig. 4b, d, e). These findings are in line with the fact that activities of PDHC and aconitase in SN56 homogenates were inhibited more strongly than those in N9 preparations (Table 3). However, sources of these differential effects of endo and exogenous NO on enzyme activities in N9 and SN56 cells remain unknown. Nevertheless, data presented here indicate that suppression of all above parameters of acetyl-CoA and energy metabolism by NO may exert weak but statistically significant impact on N9 viability, which by no means affects their cytotoxic properties (Figs 2a and d, 3a and f).

Presented data indicate for the first time the existence of substantial differences in TLR4 levels and activities of key enzymes of acetyl-CoA synthesis and utilization, as well as in energy metabolism in cholinergic neuronal and microglial cells. These factors contribute to differential distribution of acetyl-CoA/ATP in microglial and cholinergic neuronal compartments of the brain, resulting in their smaller and greater susceptibility to neurodegenerative conditions, respectively.

Acknowledgments and conflict of interest disclosure

This study was supported by Ministry of Science and Higher Education young investigator projects MN 01-0067/08 (JKŁ), MN 01-0057/08 (SGH), ST57 from Medical University of Gdańsk and POMOST C/11 programme [European Funds 2007–2013(JŁK)]. The authors have no conflicts of interest to declare.

References

Akashi S., Saitoh S. I., Wakabayashi Y. *et al.* (2003) Lipopolysaccharide interaction with cell surface Toll-like receptor 4-MD-2: higher affinity than that with MD-2 or CD14. *J. Exp. Med.* **198**, 1035–1042.

Banati R. B., Egensperger R., Maassen A., Hager G., Kreutzberg G. W. and Graeber M. B. (2004) Mitochondria in activated microglia in vitro. *J. Neurocytol.* **33**, 535–541.

Baslow M. H. (2007) N-acetylaspartate and N-acetylaspartylglutamate, in *Handbook of Neurochemistry and Molecular Biology 3rd Edition, Amino Acids and Peptides in the Nervous System* (Oja S. S., Schousboe A. and Saransaari P. eds), pp. 305–346 Springer, New York.

Beynon A. L., Brown M. R., Wright R., Rees M. I., Sheldon I. M. and Davies J. S. (2013) Ghrelin inhibits LPS-induced release of IL-6 from mouse dopaminergic neurons. *J. Neuroinflammation* **10**, 40.

Bielarczyk H. and Szutowicz A. (1989) Evidence for the regulatory function of synaptoplasmic acetyl-CoA in acetylcholine synthesis in nerve endings. *Biochem. J.* **262**, 377–380.
w?>Bielarczyk H., Jankowska-Kulawy A., Gul S., Pawełczyk T. and Szutowicz A. (2005) Phenotype dependent differential effects of interleukin-1beta and amyloid-beta on viability and choliner-gic phenotype of T17 neuroblastoma cells. *Neurochem. Int.* **47**, 466–473.

Bielarczyk H., Gul S., Ronowska A., Bizon-Zygmańska D., Pawełczyk T. and Szutowicz A. (2006) RS-alpha-lipoic acid protects cholinergic cells against sodium nitroprusside and amyloid-beta neurotoxicity through restoration of acetyl-CoA level. *J. Neurochem.* **98**, 1242–1251.

Bierer L. M., Haroutunian V., Gabriel S., Knott P. J., Carlin L. S., Purohit D. P., Perl D. P., Schmeidler J., Kanof P. and Davis K. L. (1995) Neurochemical correlates of dementia severity in Alzheimer's disease: relative importance of the cholinergic deficits. *J. Neurochem.* **64**, 749–760.

Block M. L., Zecca L. and Hong J. S. (2007) Microglia-mediated neurotoxicity: uncovering the molecular mechanism. *Nat. Rev. Neurosci.* **8**, 57–69.

Blusztajn J. K., Venturini A., Jackson D. A., Lee H. J. and Wainer B. H. (1992) Acetylcholine synthesis and release is enhanced by dibutyryl cyclic AMP in a neuronal cell line derived from mouse septum. *J. Neurosci.* **12**, 793–799.

Bradford M. (1976) A rapid sensitive method for the quantitation of microgram quantities of protein utilizing the principle of protein-dye binding. *Anal. Biochem.* **72**, 248–254.

Brown G. C. and Neher J. J. (2010) Inflammatory neurodegeneration and mechanism of microglial killing of neurons. *Mol. Neurobiol.* **41**, 242–247.

Brown G. C. and Neher J. J. (2014) Microglial phagocytosis of live neurons. *Nat. Rev. Neurosci.* **15**, 209–216.

Bubber P., Ke Z. J. and Gibson G. E. (2004) Tricarboxylic acid cycle enzymes following thiamine deficiency. *Neurochem. Int.* **45**, 1021–1028.

Bubber P., Haroutunian V., Fisch G., Blass J. P. and Gibson G. E. (2005) Mitochondrial abnormalities in Alzheimer brain: mechanistic implications. *Ann. Neurol.* **57**, 695–703.

Chen Z., Jalabi W., Shpargel K. B., Farabaugh K. T., Dutta R., Yin X., Kidd G. J., Bergmann C. C., Stohlman S. A. and Trapp B. D. (2012) Lipopolysaccharide-induced microglial activation and neuroprotection against experimental brain injury is independent of hematogenous TLR4. *Neurobiol. Dis.* **32**, 11706–11715.

Chénais B., Morjani H. and Drapier J. C. (2002) Impact of endogenous nitric oxide on microglial cell energy metabolism and labile iron pool. *J. Neurochem.* **81**, 615–623.

Cunningham C. (2013) Microglia and neurodegeneration: the role of systemic inflammation. *Glia* **61**, 71–90.

Dodd C. A. and Filipov N. M. (2011) Manganese potentiates LPS-induced heme-oxygenase 1 in microglia but not dopaminergic cells: role in controlling microglial hydrogen peroxide and inflammatory cytokine output. *Neurotoxicology* **32**, 683–692.

Fonnum F. (1975) A rapid radiochemical method for the determination of choline acetyltransferase. *J. Neurochem.* **24**, 407–409.

Gibbons H. M. and Dragunow M. (2006) Microglia induce neural cell death via a proximity-dependent mechanism involving nitric oxide. *Brain Res.* **1084**, 1–15.

Gorman M. W., Marble D. R., Ogimoto K. and Feigl E. O. (2003) Measurement of adenine nucleotides in plasma. *Luminescence* **18**, 173–181.

Hammond D. N., Lee H. J., Tonsgard J. H. and Wainer B. H. (1990) Development and characterization of clonal cell lines derived from septal cholinergic neurons. *Brain Res.* **512**, 190–200.

Hassan F., Islam S., Tumurkhuu G., Naiki Y., Koide N., Mori I., Yoshida T. and Yokoschi T. (2006) Intracellular expression of toll-like receptor 4 in neuroblastoma cells and their unresponsiveness to lipopolysaccharide. *BMC Cancer* **6**, 281.

Hines D. J., Choi H. B., Hines R. M., Phillips A. G. and MacVicar B. A. (2013) Prevention of LPS-induced microglia activation, cytokine production and sickness behavior with TLR4 receptor interfering peptides. *PLoS ONE* **8**, e60388. doi:10.1371/journal.pone.0060388.

Jankowska-Kulawy A., Bielarczyk H., Pawełczyk T., Wróblewska M. and Szutowicz A. (2010) Acetyl-CoA deficit in brain mitochondria in experimental thiamine deficiency encephalopathy. *Neurochem. Int.* **57**, 851–856.

Jin Y., Sato K., Tobo A., Mogi C., Tobo M., Murata M., Ishii S., In D. S. and Okajima F. (2014) Inhibition of interleukin-1β production by extracellular acidification though TDAG8/cAMP pathway in mouse microglia. *J. Neurochem.* **129**, 683–695.

Jung D. Y., Lee H., Jung B. Y., Ock J., Lee M. S., Lee W. H. and Suk K. (2005) TLR4, but not TLR2, signals autoregulatory apoptosis of cultured microglia: a critical role of IFN-beta as a decision maker. *J. Immunol.* **174**, 6467–6476.

Kalisch B. E., Bock N. A., Davis W. L. and Rylett R. J. (2002) Inhibitors of nitric oxide synthase attenuate nerve growth factor-mediated increases in choline acetyltransferase expression in PC12 cells. *J. Neurochem.* **81**, 624–635.

Klunk W. E., Engler H., Nordberg A. *et al.* (2004) Imaging brain amyloid in Alzheimer's disease with Pittsburgh Compound-B. *Ann. Neurol.* **55**, 306–319.

Koller K. J., Zaczek R. and Coyle J. T. (1984) N-acetyl-aspartyl-glutamate: regional levels in rat brain and the effects of brain lesions as determined by a new HPLC method. *J. Neurochem.* **43**, 1136–1142.

Lehnardt S., Massillon L., Follett P., Jensen F. E., Ratan R., Rosenberg P. A., Volpe J. J. and Vartanian T. (2003) Activation of innate immunity in the CNS triggers neurodegeneration through a Toll-like receptor 4-dependent pathway. *Proc. Natl Acad. Sci. USA* **100**, 8514–8519.

Liu B. and Hong J. S. (2003) Role of microglia in inflammation-mediated neurodegenerative diseases: mechanisms and strategies for therapeutic intervention. *J. Pharmacol. Exp. Ther.* **304**, 1–7.

Lu X., Ma L., Ruan L., Kong Y., Mou H., Zhang Z., Wang Z., Wang J. M. and Le Y. (2010) Resveratrol differentially modulates inflammatory responses of microglia and astrocytes. *J. Neuroinflammation*. **7**, 46.

Maccioni R. B., Rojo L. E., Fernandez J. A. and Kuljis R. O. (2009) The role of neuroinflammation in Alzheimer's disease. Ann. N.Y. *Acad. Sci.* **1153**, 240–246.

Machova E., Novakova J., Lisa V. and Doležal V. (2006) Docosahexanoic acid supports cell growth and expression of choline acetyltransferase and muscarinic receptors in NG108-15 cell line. *J. Mol. Neurosci.* **30**, 25–26.

McKimmie C. S., Roy D., Forster T. and Fazakerley J. K. (2006) Innate immune response gene expression profiles of N9 microglia are pathogen-type specific. *J. Neuroimmunol.* **175**, 128–141.

Moncada S. and Bolanos J. P. (2006) Nitric oxide, cell bioenergetics and neurodegeneration. *J. Neurochem.* **97**, 1676–1689.

Moss D. W. and Bates T. E. (2001) Activation of murine microglial cell lines by lipopolysaccharide and interferon-gamma causes NO-mediated decreases in mitochondrial and cellular function. *Eur. J. Neurosci.* **13**, 529–538.

Nakamura Y., Si Q. S. and Kataoka K. (1999) Lipopolysaccharide-induced microglial activation in culture: temporal profiles of morphological change and release of cytokines and nitric oxide. *Neurosci. Res.* **35**, 95–100.

Okun E., Griffioen K. J. and Mattson M. P. (2011) Toll-like receptor signaling in neural plasticity and disease. *Trends Neurosci.* **34**, 269–281.

Olesen O. F., Dago L. and Mikkelsen J. D. (1998) Amyloid β neurotoxicity in the cholinergic but not in the serotoninergic phenotype of RN46A cells. *Mol. Brain Res.* **57**, 266–274.

O'Neill L. A. and Hardie D. G. (2013) Metabolism of inflammation limited by AMPK and pseudo-starvation. *Nature* **493**, 346–355.

Pappas B. A., Bayley P. J., Bui B. K., Hansen L. A. and Thal L. J. (2000) Choline acetyltransferase activity and cognitive domain scores of Alzheimer's patients. *Neurobiol. Aging* **21**, 11–17.

Park C. H., Zang H., Sheu K. F. R., Calingasan N. Y., Kristal B. S., Lindsay J. G. and Gibson G. E. (1999) Metabolic impairment induces oxidative stress, compromises inflammatory responses, and inactivates a key mitochondrial enzyme in microglia. *J. Neurochem.* **72**, 1948–1958.

Persson M. and Ronnback L. (2012) Microglia self-defence mediated through GLT-1 and glutathione. *Amino Acids* **42**, 207–219.

Reynolds S. F. and Blass J. P. (1975) Normal level of acetyl coenzyme A and of acetylcholine in the brains of thiamine-deficient rats. *J. Neurochem.* **34**, 185–186.

Ronowska A., Dyś A., Jankowska-Kulawy A., Klimaszewska-Łata J., Bielarczyk H., Romianowski P., Pawełczyk T. and Szutowicz A. (2010) Short-term effects of zinc on acetylcholine metabolism and viability of SN56 cholinergic neuroblastoma cells. *Neurochem. Int.* **56**, 143–151.

Schubert P., Ogata T., Marchini C. and Ferroni S. (2001) Glia-related pathomechanisms in Alzheimer's disease: a therapeutic target? *Mech. Ageing Dev.* **123**, 47–57.

Sensi S. L., Paoletti P., Bush A. I. and Sekler I. (2009) Zinc in the physiology and pathology of the CNS. *Nat. Rev. Neurosci.* **10**, 780–792.

Sheu K. F. R., Kim Y. T. and Blass J. P. (1985) An immunological study of the pyruvate dehydrogenase deficit in Alzheimer's disease brain. *Ann. Neurol.* **17**, 444–449.

Spector D. L., Goldman R. D. and Leinwand L. A. (eds) (1998) *Cell Laboratory Manual I: Culture and Biochemical Analysis of Cells*. pp. 2.8–2.13 Cold Spring Harbor, NY.

Szutowicz A. and Bielarczyk H. (1987) Elimination of CoASH interference from acetyl-CoA assay by maleic anhydride. *Anal. Biochem.* **164**, 292–296.

Szutowicz A., Stępień M. and Piec G. (1981) Determination of pyruvate dehydrogenase and acetyl-CoA synthetase activities using citrate synthase. *Anal. Biochem.* **115**, 81–87.

Szutowicz A., Tomaszewicz M. and Bielarczyk H. (1996) Disturbances of acetyl-CoA, energy and acetylcholine metabolism in some encephalopathies. *Acta Neurobiol. Exp.* **56**, 323–339.

Szutowicz A., Tomaszewicz M., Bielarczyk H. and Jankowska A. (1998) Putative significance of shifts in acetyl-CoA compartmentalization in nerve terminals for disturbances of cholinergic transmission in brain. *Dev. Neurosci.* **20**, 485–492.

Szutowicz A., Jankowska A., Blusztajn J. K. and Tomaszewicz M. (1999) Acetylcholine and acetyl-CoA metabolism in differentiating SN56 septal cell line. *J. Neurosci. Res.* **57**, 131–136.

Szutowicz A., Madziar B., Pawełczyk T., Tomaszewicz M. and Bielarczyk H. (2004) Effects of NGF on acetylcholine, acetyl-CoA metabolism, and viability of differentiated and non-differentiated cholinergic neuroblastoma cells. *J. Neurochem.* **90**, 952–961.

Szutowicz A., Bielarczyk H., Gul S., Ronowska A., Pawełczyk T. and Jankowska-Kulawy A. (2006) Phenotype-dependent susceptibility of cholinergic neuroblastoma cells to neurotoxic inputs. *Metab. Brain Dis.* **21**, 149–161.

Szutowicz A., Bielarczyk H., Jankowska-Kulawy A., Pawełczyk T. and Ronowska A. (2013) Acetyl-CoA the key factor for survival or death of cholinergic neurons in course of neurodegenerative diseases. *Neurochem. Res.* **38**, 1523–1542.

Tomaszewicz M., Rossner S., Schliebs R., Ćwikowska J. and Szutowicz A. (2003) Changes incortical acetyl-CoA metabolism after selective basal forebrain cholinergic degeneration by 192IgG-saporin. *J. Neurochem.* **87**, 318–324.

Tuček S. (1993) Short-term control of the synthesis of acetylcholine. *Prog. Biophys. Mol. Biol.* **60**, 59–69.

Vaisid T. and Kosower N. S. (2013) Calpastatin is upregulated in non-immune neuronal cells via toll-like receptor 2 (TLR2) pathways by lipid-containing agonists. *Biochim. Biophys. Acta* **1833**, 2369–2377.

Visintin A., Mazzoni A., Spitzer J. A. and Segal D. M. (2001) Secreted MD-2 is a large polymeric protein that efficiently confers lipopolysaccharide sensitivity to Toll-like receptor 4. *Proc. Natl Acad. Sci. USA* **98**, 12156–12161.

Welser-Alves J. and Milner R. (2013) Microglia are the major source of TNF-α and TGF-β1 in postnatal glial cultures: regulation by cytokines, lipopolysaccharide and vitronectin. *Neurochem. Int.* **63**, 47–53.

Xie Z., Wei M., Morgan T. E., Fabrizio P., Han D., Finch C. E. and Longo V. D. (2002) Peroxynitrite mediates neurotoxicity of amyloid beta-peptide1-42- and lipopolysaccharide-activated microglia. *J. Neurosci.* **22**, 3484–3492.

Ye J., Liu Z., Wei J., Lu L., Huang Y., Luo L. and Xie H. (2013) Protective effect of SIRT1 on toxicity of microglial-derived factors by LPS to PC12 cells via the p53-caspase-3-dependent apoptotic pathway. *Neurosci. Lett.* **553**, 72–77.

Zaidi N., Swinnen J. V. and Smans K. (2012) ATP-citrate lyase: a key player in cancer metabolism. *Cancer Res.* **72**, 3709–3714.

Zhao M., Zhou A., Xu L. and Zhang X. (2014) The role of TLR4-mediated PTEN/PI3K/AKT/NF-κB signaling pathway in neuroinflammation in hippocampal neurons. *Neuroscience* **269**, 93–101.